Hindawi Publishing Corporation
Journal of Nanomaterials
Volume 2014, Article ID 943796, 10 pages
http://dx.doi.org/10.1155/2014/943796

Research Article

Enhanced Photocatalytic Activity of W-Doped and W-La-Codoped TiO_2 Nanomaterials under Simulated Sunlight

Chenghe Hua,[1] Xiaoli Dong,[1] Xiuying Wang,[2] Mang Xue,[1] Xiufang Zhang,[1] and Hongchao Ma[1]

[1] *School of Light Industry and Chemical Engineering, Dalian Polytechnic University, No. 1 Qinggongyuan, Dalian 116034, China*
[2] *Instrumental Analysis Center, Dalian Polytechnic University, No. 1 Qinggongyuan, Dalian 116034, China*

Correspondence should be addressed to Xiaoli Dong; dongxiaoli65@163.com

Received 10 July 2014; Revised 29 August 2014; Accepted 30 August 2014; Published 21 October 2014

Academic Editor: Yuekun Lai

W-doped TiO_2 and W-La-codoped TiO_2 nanomaterials were successfully synthesized via the sol-gel method. The products were characterized by X-ray diffraction, UV-vis diffuse reflectance spectrophotometer, transmission electron microscopy, and X-ray photoelectron spectroscopy. The presence of W and La results in significant red shift of absorption edge for TiO_2-based nanomaterials. The weight ratios of La and W in the composites play important roles in the absorption edge for TiO_2-based nanomaterials. The photocatalytic activities of both W-doped TiO_2 and W-La-codoped TiO_2 photocatalysts for decolorization of methyl orange solution were evaluated under simulated sunlight irradiation. The results showed that both W-doped and W-La-codoped can effectively improve the photocatalytic behaviors of TiO_2 nanomaterials ascribed to the improved photoinduced charge carriers separation, enhanced light absorption, and large surface area. Furthermore, W-La-codoped TiO_2 exhibited higher photocatalytic activity than W-doped TiO_2. Considering their high photocatalytic activity, the doped TiO_2 nanomaterials could be applied in wastewater treatment and environmental purification.

1. Introduction

Nowadays, in view of the increasing awareness on environmental pollution, application of semiconductor photocatalysis for chemical wastes treatment has been considered as a promising approach and attracted extensive attention [1–10]. A series of semiconductors has been successfully used as photocatalysts, including oxides and sulfides [11–16]. Among these semiconductors, TiO_2 is especially attractive because of its high photocatalytic activity, excellent chemical stability, nontoxicity, and low cost, making it potentially suitable for conversion of solar energy to electricity or chemical energy [17–21]. However, TiO_2 with large energy bandgap of 3.2 eV can be only excited by UV light, which merely occupies about 4% of solar energy. It leads to the less utilization of solar energy and inhibits the practical application of TiO_2 under sunlight. Aiming at solving this shortcoming, many approaches have been successfully reported to make TiO_2-based materials respond to visible light, such as composite semiconductors, transition metal doping, and noble metal deposition [22–29]. Among these methods, transition metal doping is usually considered to be one of the most effective strategies for improving the photocatalytic activity of TiO_2 under visible light. The construction of doped TiO_2 materials introduces additional electronic states within the bandgap, leading to an extension of light absorption in the visible region. In addition, doped TiO_2 materials increase the lifetime of photoinduced charge carriers by bandgap irradiation, thereby leading to enhancement of photocatalytic efficiency [25]. Palmisano has investigated the influence of a series of transition metal ions (Co, Cr, Cu, Fe, Mo, V, and W) on the photocatalytic activity of TiO_2. The results show that only W-doping distinctly enhances the photocatalytic activity of TiO_2 under visible light irradiation [26]. In addition, rare earth metals can also be used to enhance the visible light photocatalytic activity of TiO_2 [30–34]. Although single metal ion doped TiO_2 has been widely investigated, the utilization of two-metal-ion codoped TiO_2 as a visible light photocatalyst has not been adequately investigated.

In this paper, both W-doped and W-La-codoped TiO_2 nanomaterials have been successfully synthesized via a sol-gel method. The results show that the existence of W and La in the nanomaterials can effectively enhance the photocatalytic behaviors of TiO_2 for decolorization of methyl orange solution under simulated sunlight irradiation. It is mainly attributed to the improved photoinduced charge carriers separation, enhanced light absorption, and large surface area.

2. Experimental Section

2.1. Materials. Anhydrous ethanol (C_2H_5OH, AR), tetrabutyl titanate (TBOT, CP), acetic acid (CH_3COOH, AR), ammonium tungstate hydrate ($(NH_4)_{10}W_{12}O_{41} \cdot xH_2O$, AR), lanthanum nitrate hexahydrate ($La(NO_3)_3 \cdot 6H_2O$, AR), methyl orange (MO, AR), and nitric acid (HNO_3, GR, 65–68 wt%) were used without further purification.

2.2. Preparation of W-Doped TiO_2 Nanomaterials. Firstly, a sol-gel solution, denoted by solution A, was prepared by dispersing 17 mL of TBOT and 0.2 mL of HNO_3 in 40 mL of C_2H_5OH with ultrasonic vibration for 30 min. Another solution, denoted by solution B, was prepared by mixing 4 mL of deionized water, 5 mL of CH_3COOH, and 20 mL of C_2H_5OH. Then, solution B was added dropwise into solution A under vigorous stirring. Subsequently, a certain amount of $(NH_4)_{10}W_{12}O_{41}$ solution with the concentration of 20 mg·L^{-1} was added to the above solution under vigorous stirring. The solution was aged at room temperature for 5 h and the precursor gel was obtained. Finally, the gel was dried at 100°C for 6 h, grinded, and calcined at 400°C for 3 h in air. The weight ratio of W in the catalysts could be easily controlled by adjusting the amount of $(NH_4)_{10}W_{12}O_{41}$ solution. The obtained samples with different weight ratio of W to Ti (0, 0.4%, 0.6%, 0.8%, 1%, and 1.2%) were denoted by TiO_2, 0.4% W/TiO_2, 0.6% W/TiO_2, 0.8% W/TiO_2, 1.0% W/TiO_2, and 1.2% W/TiO_2, respectively.

2.3. Preparation of W-La-Codoped TiO_2 Nanomaterials. The synthesis of *W-La-codoped TiO_2 nanomaterials* was similar to that of 0.8% W/TiO_2 nanomaterials, except that solution B was added to different amount of $La(NO_3)_3 \cdot 6H_2O$ to make the weight ratio of La to Ti be 1%, 2%, 3%, 4%, and 5%. These samples were denoted by 1% La/W/TiO_2, 2% La/W/TiO_2, 3% La/W/TiO_2, 4% La/W/TiO_2, and 5% La/W/TiO_2, respectively.

2.4. Characterization. The samples were examined by X-ray diffraction (XRD) on a Shimadzu XRD-6100 diffractometer with Cu Kα radiation (λ = 0.154 nm), operating at 40 kV and 100 mA. The diffused reflectance UV-visible spectra (DRS) were recorded on a CARY 100 CONC spectrometer. Transmission electron microscopy (TEM) was carried out with a JEOL JEM-2000EX operating at 200 kV. X-ray photoelectron spectra (XPS) were recorded with a VG Scientific ESCALAB250 XPS instrument. The C(1s) level was used as an internal reference at 284.6 eV. Energy dispersive X-ray spectroscopy (EDS) was recorded with Oxford INCA. The N_2 adsorption-desorption was measured by JW-BK222 nitrogen adsorption analyzer. Photoluminescence (PL) spectra were recorded by fluorescence spectroscopy (LS55) with the excitation wavelength of 280 nm.

2.5. Photocatalytic Decolorization of MO Solution. The photocatalytic activities were evaluated by photodecolorization of MO solution with pH = 3.0 at 30°C. In this case, a 350 W xenon lamp was used as a light source. 200 mg of photocatalyst was added to 200 mL of MO solution with the initial concentration of 20 mg · L^{-1} and then magnetically stirred in the dark for 20 min to ensure the establishment of an adsorption-desorption equilibrium and uniform distribution. The suspensions were collected every 20 min and centrifuged to separate the photocatalyst particles. The MO concentration was determined by monitoring the absorbance peak at λ_{max} = 464 nm using a Shimadzu, UV-1600 (PC) UV-visible spectrophotometer.

3. Results and Discussion

Figure 1 shows the XRD patterns of the as-synthesized W-doped TiO_2 and W-La-codoped TiO_2. It can be seen that all of the diffraction peaks are ascribed to anatase TiO_2 and no peaks indexed to WO_3 and La_2O_3 are detected, indicating that crystalline WO_3 and La_2O_3 are not formed in this case. According to previous report [35], W^{6+} should be present in substitutional positions of Ti^{4+} in the lattice of TiO_2 due to the similar ionic radii between W^{6+} and Ti^{4+}. However, it seems difficult for La^{3+} to be incorporated into the lattice of TiO_2 due to the mismatch of the ionic radii of Ti^{4+} and La^{3+}, and it may exist in the form of La_2O_3 which was very small and highly dispersed in the composites [31, 36]. In addition, the broadened peaks suggest that the samples are composed of nanosized particles.

XPS analysis is performed to identify the chemical composition of the W-La-codoped TiO_2. The XPS spectrum for 4% La/W/TiO_2 shown in Figure 2(a) displays the corresponding peaks of O1s, Ti2p, C1s, W4f, and La3d, indicating the existence of W and La in the composite. The spectrum in Figure 2(b) shows two peaks locating at 458.9 and 464.4 eV, arising from the spin-orbit splitting of the Ti2p components, namely, $Ti2p_{3/2}$ and $Ti2p_{1/2}$, which are in good agreement with those of titanium dioxide [37]. Figure 2(c) exhibits the $W4f_{7/2}$ core level binding energy peak at 36.7 eV, which is consistent with that of tungsten trioxide [38]. The weak peak located at 835 eV in Figure 2(d) is related to La3d components ($La3d_{5/2}$). For further confirming the existence of W and La, EDS has also been performed (Figure 3). It can be clearly seen that the signals for W are present in W-doped TiO_2 nanomaterials, and the weight ratio of W/Ti is consistent with what we proposed. Similarly, W and La signals also appeared in the EDS spectrum of W-La-codoped TiO_2, illustrating the existence of W and La.

In order to study the morphology of the obtained samples, TEM is performed. As shown in Figure 4(a), pure TiO_2 are composed of small nanoparticles with the diameter in the

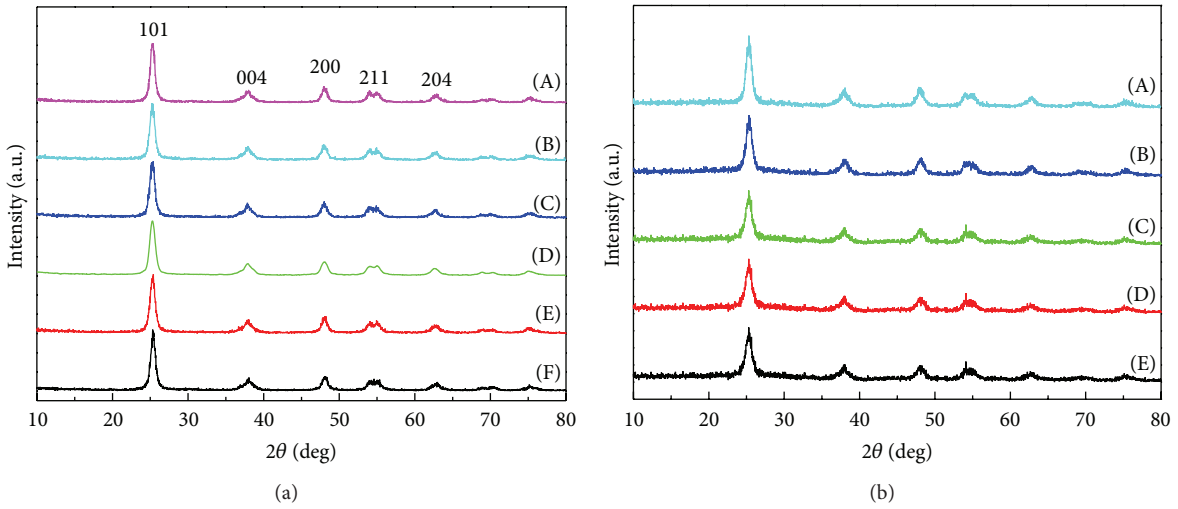

FIGURE 1: XRD patterns of (A) pure TiO_2, (B) 0.4% W/TiO_2, (C) 0.6% W/TiO_2, (D) 0.8% W/TiO_2, (E) 1.0% W/TiO_2, and (F) 1.2% W/TiO_2 in (a) and (A) 1% $La/W/TiO_2$, (B) 2% $La/W/TiO_2$, (C) 3% $La/W/TiO_2$, (D) 4% $La/W/TiO_2$, and (E) 5% $La/W/TiO_2$ in (b).

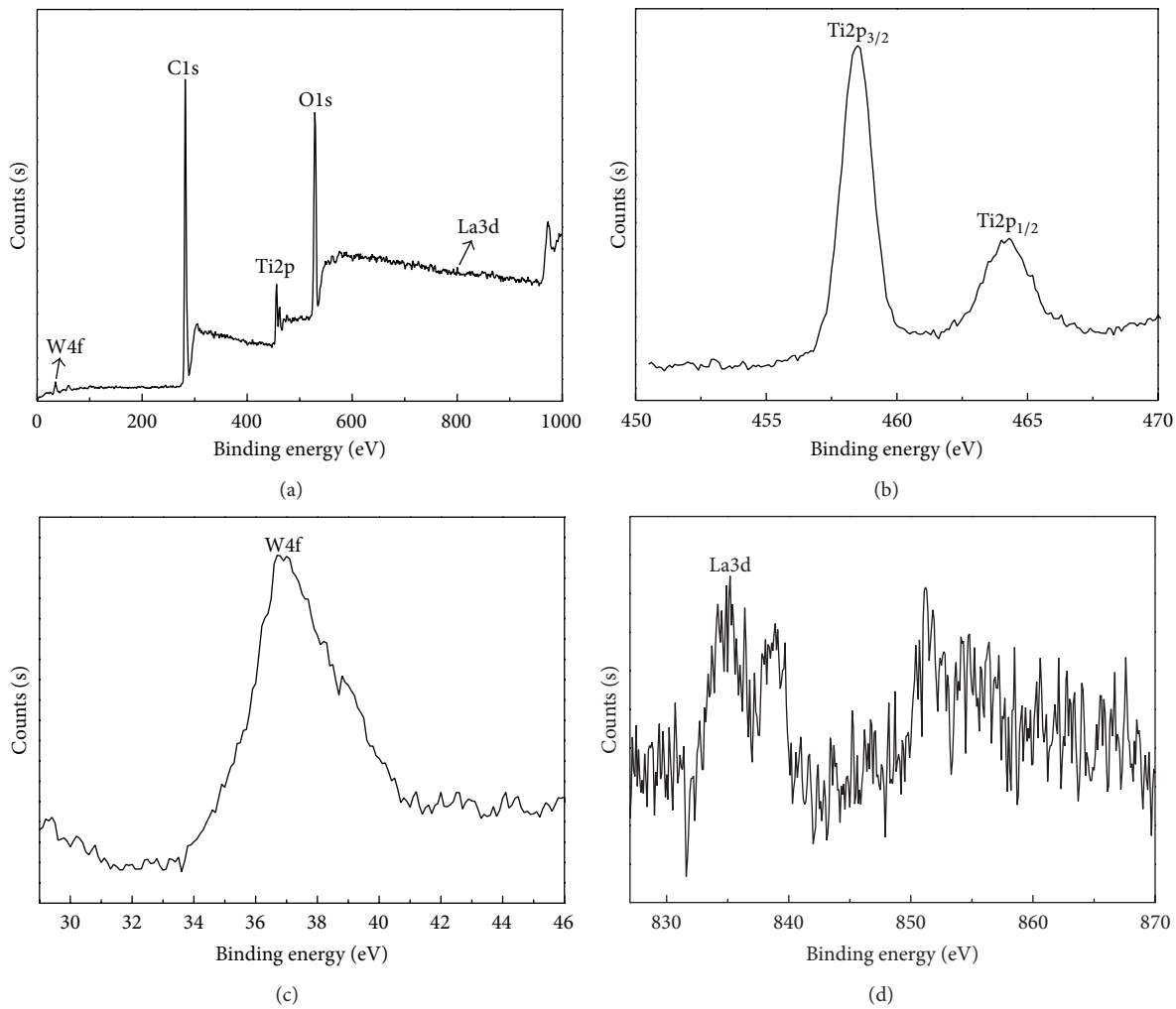

FIGURE 2: The XPS core level binding energy in the 4% $La/W/TiO_2$ nanomaterials. (a) An overview XPS spectrum of the sample; (b) Ti2p spectrum; (c) W4f spectrum; and (d) La5/2d spectrum.

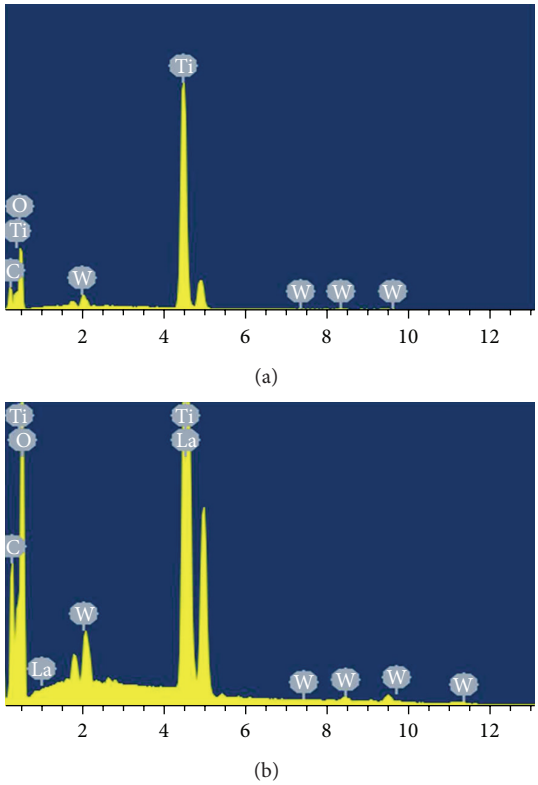

FIGURE 3: EDS spectra of the (a) 0.8% W/TiO_2 and (b) 4% La/W/TiO_2 nanomaterials, respectively.

range of 15–30 nm. However, both W-doped TiO_2 and W-La-codoped TiO_2 consist of small nanoparticles, which are uniform with the main diameter of approximately 10 and 8 nm, respectively. It is attributed to the presence of W and La in the composites, which can inhibit the growth of TiO_2 nanoparticles [36, 39, 40]. This is well consistent with the results of XRD studies. In HRTEM image, the fringe spacing of 0.35 nm can be indexed to the (101) plane of anatase TiO_2, indicating well crystalline TiO_2 nanoparticles are formed in this case.

Figure 5(a) shows the UV-vis absorption spectra of the TiO_2 and W-doped TiO_2 nanomaterials with various amounts of W, converted from the corresponding diffuse reflectance spectra. It can be seen that pure TiO_2 nanomaterials only exhibit the fundamental absorption band in the UV light region, while the absorption edge shifts towards visible light region obviously for the W-doped TiO_2 materials. Furthermore, a gradual red shift of absorption edge is noticed along with increasing the amount of W, when the amount of W is smaller than 0.8%. The absorption of the UV light in TiO_2 is ascribed to the excitation of the O2p electron to the Ti3d level [41]. The red-shifted absorption edge for W-doped TiO_2 may be associated with the charge transfer between TiO_2 valence or conduction band and W ion level. It implies that the bandgap of TiO_2 can be adjusted by the trapping level, which is formed through doping with appropriate metal ions. It has been reported that the existence of La can also result in the red shift of absorption range of TiO_2 to visible light region [42]. As shown in Figure 5(a), it is also found that the absorption edge of 4% La/W/TiO_2 is red-shifted compared with that of 0.8% W/TiO_2. The bandgaps estimated from the plots of $(F(R)h\nu)^2$ versus photon energy $h\nu$ are presented in Figure 5(b) and it is apparent W-doping and La-doping lead to the decrease of bandgap of TiO_2 from 3.19 to 3.10 eV, indicating that the obtained TiO_2 nanomaterials display the visible light response. They are anticipated to exhibit better photochemical activity under visible light.

In order to further investigate the texture of the obtained composites, N_2 adsorption/desorption measurements are conducted. Figure 6(a) shows the nitrogen adsorption-desorption isotherms of pure TiO_2, W-doped TiO_2, and W-La-codoped TiO_2 nanomaterials. The isotherms are characteristic of type-IV curves, indicating the presence of mesoporosity in the synthesized materials. Figure 6(b) shows the pore size distributions of pure TiO_2, W-doped TiO_2, and W-La-codoped TiO_2. It is clearly seen that the pores in pure TiO_2 have the diameter of about 4 nm, whereas the majority of pores in W-doped TiO_2 and W-La-codoped TiO_2 are around 2 nm. However, it should be noted that some mesopores with the diameter of 5 nm are present in W-doped TiO_2. The BET specific surface areas of pure TiO_2, W-doped TiO_2, and W-La-codoped TiO_2 are 5.0, 86.3, and 102.7 $m^2 \cdot g^{-1}$. The higher specific surface areas of W-doped TiO_2 and W-La-codoped TiO_2 are ascribed to the smaller particle size. For comparison, P25 is also characterized by N_2 adsorption/desorption measurement. The BET specific surface area is 42.8 $m^2 \cdot g^{-1}$ and the main diameter of pores is approximately 2 nm.

The photocatalytic activity of the W-doped TiO_2 nanocrystals is evaluated by photodecolorization of MO solution, which is a typical azo dye and difficult to be degraded. Figure 7(a) presents the adsorption effect of pure TiO_2, 0.8% W/TiO_2, and 4% La/W/TiO_2 on MO in the dark. The adsorption equilibrium is reached for all three samples after 20 min. It is obvious that the adsorption capacity of 4% La/W/TiO_2 is superior to those of pure TiO_2 and 0.8% W/TiO_2, due to the large specific surface area of 4% La/W/TiO_2. Figure 7(b) presents the photocatalytic performance for the decolorization efficiency of MO solution in the presence of P25, pure TiO_2, and W-doped TiO_2 nanocrystals. It is clear that all of the W-doped TiO_2 nanomaterials exhibit higher photocatalytic activity than that of pure TiO_2 and P25, which possess the similar porous structures. This is attributed to improved photoinduced charge carriers separation, enhanced light absorption, and large surface area. Under simulated sunlight irradiation, the electrons in the TiO_2 structures can be easily excited from the valence band into the conduction band. Then the excited electrons in the conduction band probably transfer to the W ion states and the holes are left in the valence band [35]. Subsequently, the charge carriers transfer to the surface of photocatalyst and initiate the oxidation of MO. In addition, W-doping increases the light absorption owing to the red shift of absorption range to the visible light region. Meanwhile, the surface area is also important for photocatalytic activity. Comparing with the pure TiO_2 and P25, 0.8% W/TiO_2 nanomaterials display a

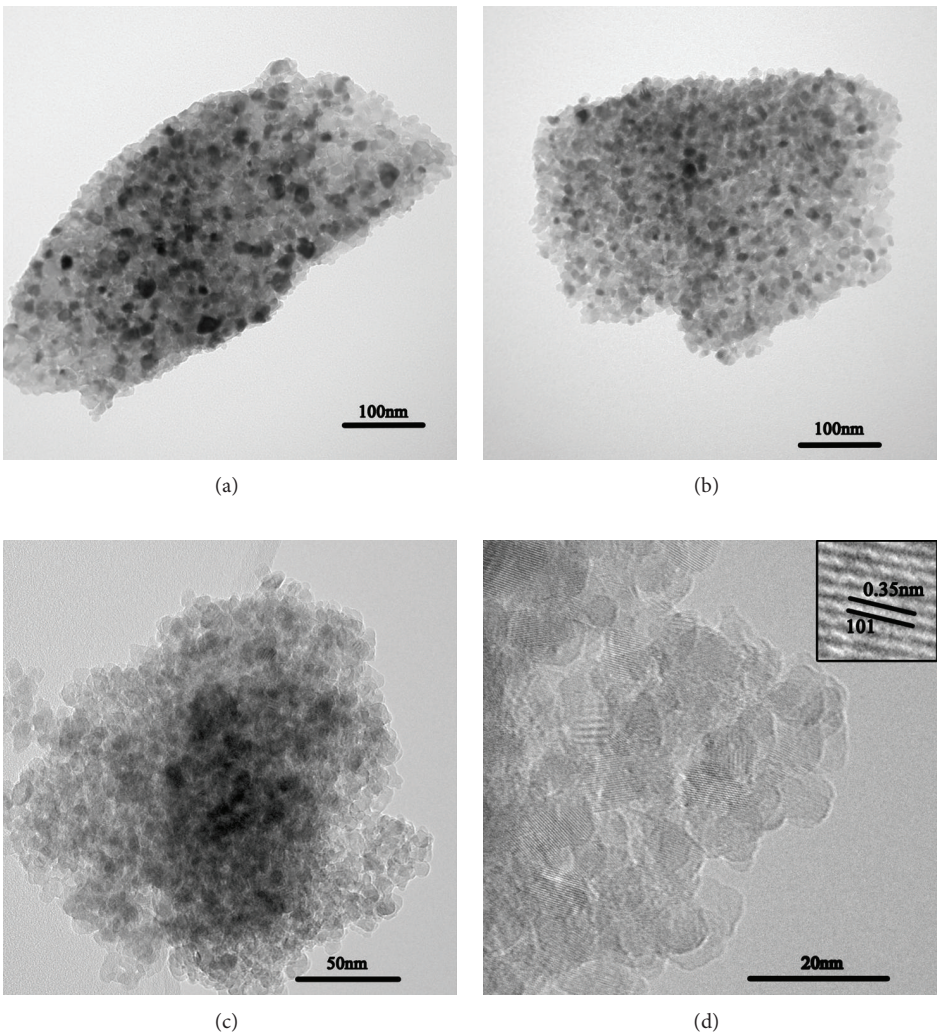

(a) (b) (c) (d)

Figure 4: TEM images of (a) pure TiO_2, (b) 0.8% W/TiO_2, and (c) 4% $La/W/TiO_2$ nanomaterials. (d) The high-resolution TEM (HRTEM) image of 4% $La/W/TiO_2$ nanomaterials.

larger surface area, giving birth to more contact area during photocatalystic reaction. All of above advantages make 0.8% W/TiO_2 nanomaterials present higher photocatalytic activity. It should be noted that the decolorization efficiency increases with increasing of the amount of W as long as it is smaller than 0.8%. Further increasing the dopant content results in the decrease of decolorization efficiency. It may be attributed to that W ions begin to act as recombination centers for the photogenerated electrons and holes, when the amount of W is larger than 0.8%. So the decolorization efficiency is dramatically decreased. Figure 7(c) displays the decolorization efficiency of MO over the as-synthesized products under simulated sunlight irradiation. It is obvious that the decolorization efficiency increases to 67.4% along with the increase of La-doping amount to 4%. Similar to W-doped TiO_2, further increasing the amount of La results in the decrease of decolorization efficiency. And all of the W-La-codoped TiO_2 nanomaterials exhibit higher photocatalytic activity than those of W-doped TiO_2 nanomaterials. According to previous report [31], La_2O_3 on the surface of TiO_2 may favor the separation of charge carriers and prolong the life of carriers. In addition, the existence of La_2O_3 can also increase the amount of hydroxyl radicals on the surface of the photocatalyst, available for oxidation of MO. As a result, the presence of La enhances the photocatalytic activity of W-La-codoped TiO_2 nanomaterials. The efficient charge separation in the W-doped TiO_2 and W-La-codoped nanomaterials is confirmed by PL spectra. As observed in Figure 7(d), 0.8% W/TiO_2 exhibits much lower emission intensity than that of pure TiO_2 nanomaterials, indicating that the recombination of the photoinduced charge carrier is greatly inhibited in 0.8% W/TiO_2 nanomaterials. It can also be found that W-La-codoped TiO_2 presents apparent quenching of the W-doped TiO_2 fluorescence, which indicates the suppression of the recombination of electrons and holes.

The recycling performance is known as one of the main methods for describing the role of catalysts in practical applications. Figure 8 shows the recycling behaviors of 0.8%

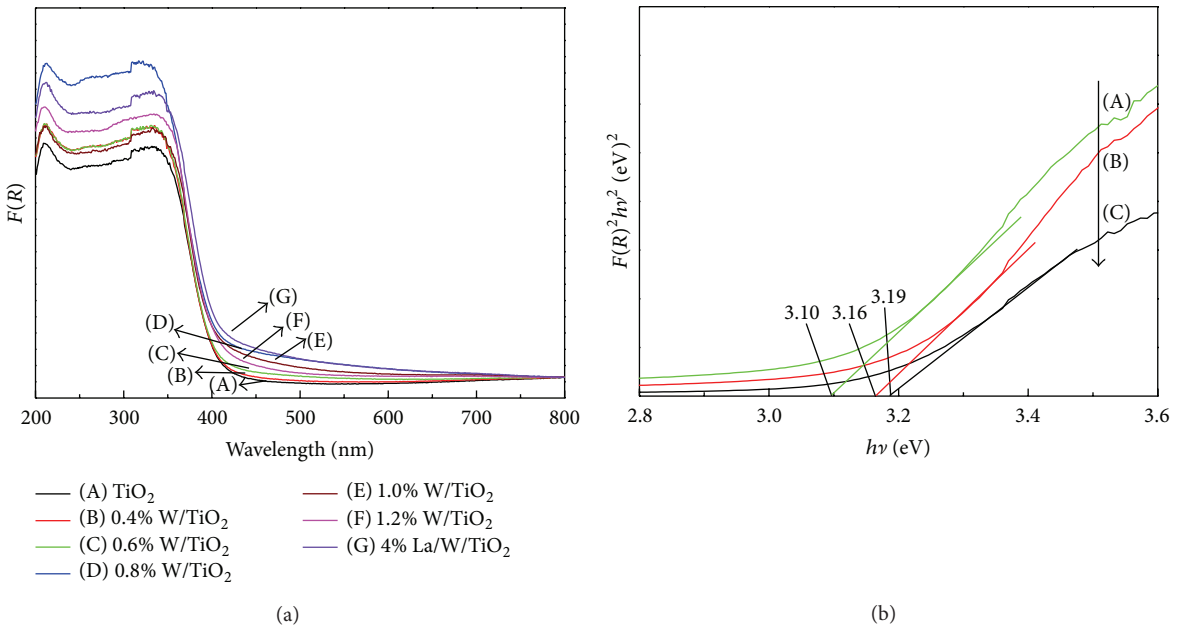

FIGURE 5: (a) UV-vis absorption spectra of the pure TiO_2, W-doped TiO_2 with different W content and 4% La/W/TiO_2 nanomaterials and (b) $(F(R)h\nu)^2$ versus $h\nu$ plots of (A) 4% La/W/TiO_2, (B) 0.8% W/TiO_2, and (C) pure TiO_2 nanomaterials.

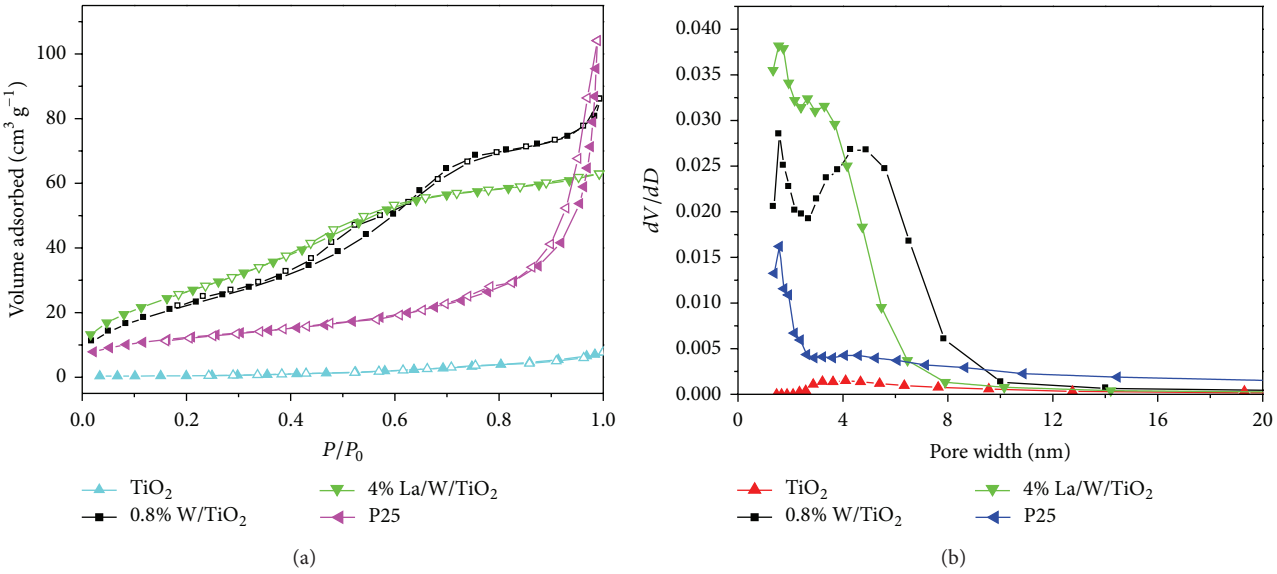

FIGURE 6: N_2 adsorption-desorption (a) isotherms and (b) pore size distribution plot.

W/TiO_2 and 4% La/W/TiO_2 for decolorization of MO. It is seen that the decolorization efficiency of MO using 0.8% W/TiO_2 and 4% La/W/TiO_2 reaches 45.0% and 67.4% in the first cycle. After five cycles, the decolorization efficiency of MO on 0.8% W/TiO_2 and 4% La/W/TiO_2 is 42.8 and 65.1%, respectively, indicating both 0.8% W/TiO_2 and 4% La/W/TiO_2 possess superior recycling ability.

In order to get a better comparison of the photocatalytic activities of the doped TiO_2 nanomaterials, the kinetic analysis of decolorization of MO is also discussed. As shown in Figure 9, the kinetic linear simulation curves of the photocatalytic decolorization of MO solution in the presence of different photocatalysts show that all the decolorization reactions can be described by first-order reaction dynamics due to the low initial concentration of the MO solution ($20\,mg \cdot L^{-1}$ in this case). Meanwhile, the slopes of these lines suggest the reaction rate constant of 4% La/W/TiO_2 is larger than any other sample in this case, implying 4% La/W/TiO_2 nanomaterials possess the highest photocatalytic activity.

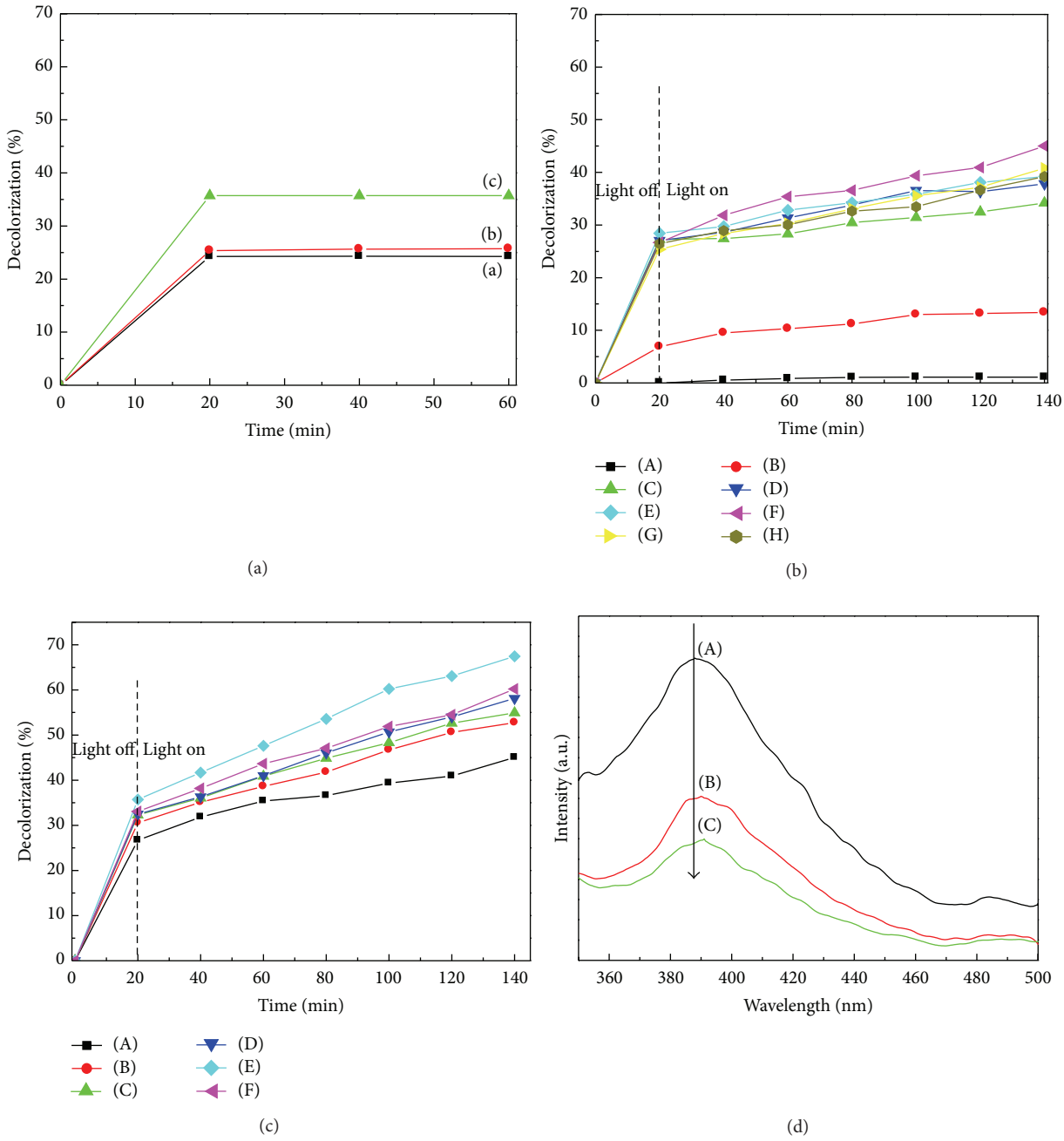

FIGURE 7: (a) Decolorization profiles of MO in the presence of (A) pure TiO_2, (B) 0.8% W/TiO_2, and (C) 4% $La/W/TiO_2$ in the dark. Photocatalytic decolorization curves of MO over the catalysts under simulated sunlight irradiation: (A) blank, (B) P25, (C) pure TiO_2, (D) 0.4% W/TiO_2, (E) 0.6% W/TiO_2, (F) 0.8% W/TiO_2, (G) 1.0% W/TiO_2, and (H) 1.2% W/TiO_2 in (b) and (A) 0.8% W/TiO_2, (B) 1% $La/W/TiO_2$, (C) 2% $La/W/TiO_2$, (D) 3% $La/W/TiO_2$, (E) 4% $La/W/TiO_2$, and (F) 5% $La/W/TiO_2$ in (c). (d) PL spectra of the (A) pure TiO_2, (B) 0.8% W/TiO_2, and (C) 4% $La/W/TiO_2$ nanomaterials.

4. Conclusions

In summary, the W-doped TiO_2 and W-La-codoped TiO_2 nanomaterials are prepared through a sol-gel method. The presence of W and La results in red shift of absorption edge for TiO_2 nanomaterials. The investigation of photocatalytic activity indicates the W-doped and La-doped can effectively improve the photocatalytic activity of TiO_2 under simulated sunlight irradiation due to improved photoinduced charge carriers separation, enhanced light absorption, and large

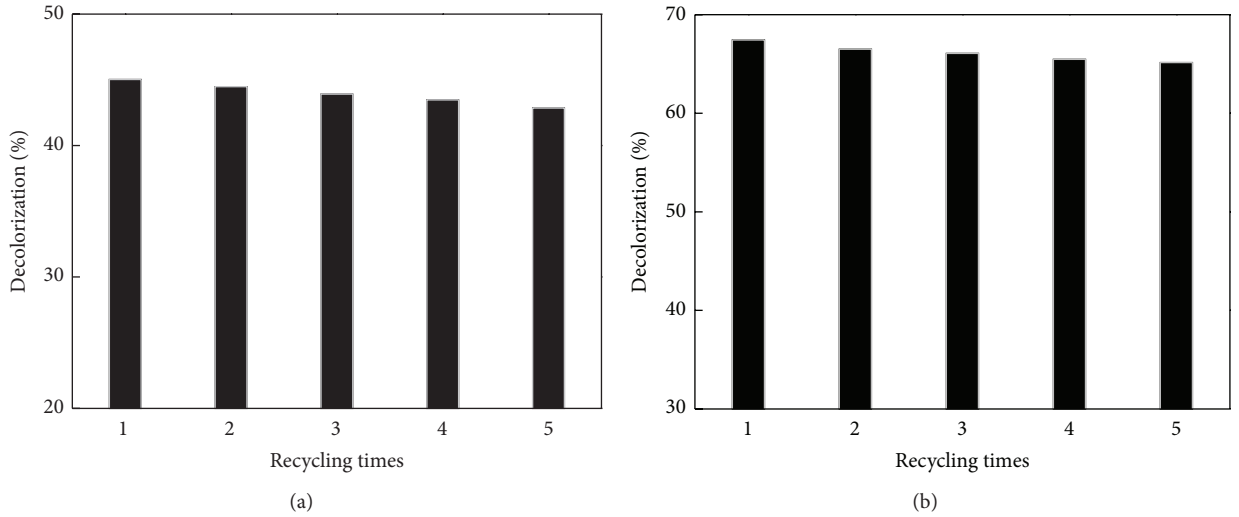

FIGURE 8: (A) Decolorization curves of MO over (a) 0.8% W/TiO_2 and (b) 4% La/W/TiO_2 nanomaterials for reusing 5 times.

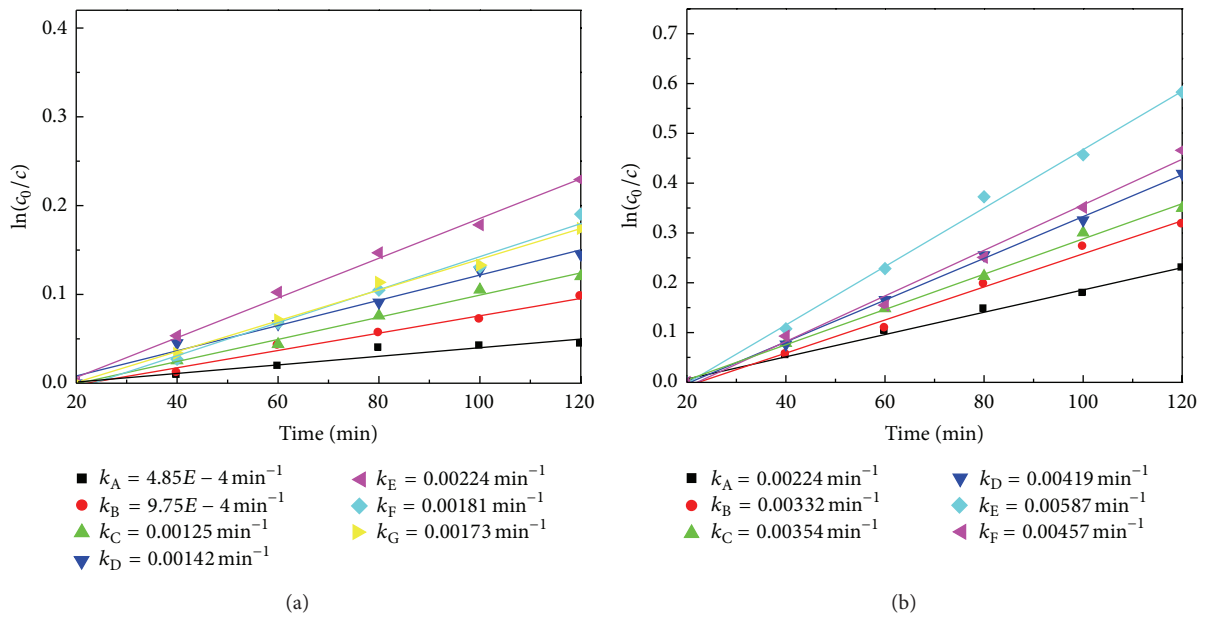

FIGURE 9: Kinetic linear simulation curves of MO photocatalytic decolorization over the different photocatalysts under simulated sunlight irradiation: (A) p25, (B) pure TiO_2, (C) 0.4% W/TiO_2, (D) 0.6% W/TiO_2, (E) 0.8% W/TiO_2, (F) 1.0% W/TiO_2, and (G) 1.2% W/TiO_2 in (a) and (A) 0.8% W/TiO_2, (B) 1% La/W/TiO_2, (C) 2% La/W/TiO_2, (D) 3% La/W/TiO_2, (E) 4% La/W/TiO_2, and (F) 5% La/W/TiO_2 in (b). c_0 and c are the MO concentration when adsorption equilibrium is reached and at time t, respectively.

surface area. Considering their high photocatalytic activity, the doped TiO_2 nanomaterials can be applied in wastewater treatment and environmental purification.

Conflict of Interests

The authors declare that there is no conflict of interests regarding the publication of this paper.

Acknowledgments

The research was supported by Program for Key Science & Technology Platform ([2011]191) in Universities of Liaoning Province, the National Natural Science Foundation of China (Grant no. 21476033), and Cultivation Program for Excellent Talents of Science and Technology Department of Liaoning Province (no. 201402610).

References

[1] J. Hoigne and H. Bader, "The role of hydroxyl radical reactions in ozonation processes in aqueous solutions," *Water Research*, vol. 10, no. 5, pp. 377–386, 1976.

[2] S. Rasalingam, R. Peng, and R. T. Koodali, "Removal of hazardous pollutants from wastewaters: applications of TiO_2-SiO_2 mixed oxide materials," *Journal of Nanomaterials*, vol. 2014, Article ID 617405, 42 pages, 2014.

[3] J. Li, L. Gao, Q. Zhang et al., "Photocatalytic property of $Fe_3O_4/SiO_2/TiO_2$ core-shell nanoparticle with different functional layer thicknesses," *Journal of Nanomaterials*, vol. 2014, Article ID 986809, 7 pages, 2014.

[4] Q.-P. Luo, X.-Y. Yu, B.-X. Lei, H.-Y. Chen, D.-B. Kuang, and C.-Y. Su, "Reduced graphene oxide-hierarchical ZnO hollow sphere composites with enhanced photocurrent and photocatalytic activity," *The Journal of Physical Chemistry C*, vol. 116, no. 14, pp. 8111–8117, 2012.

[5] L. Andronic, D. Andrasi, A. Enesca, M. Visa, and A. Duta, "The influence of titanium dioxide phase composition on dyes photocatalysis," *Journal of Sol-Gel Science and Technology*, vol. 58, no. 1, pp. 201–208, 2011.

[6] Y. A. Cao, W. S. Yang, W. F. Zhang, G. Z. Liu, and P. Yue, "Improved photocatalytic activity of Sn^{4+} doped TiO_2 nanoparticulate films prepared by plasma-enhanced chemical vapor deposition," *New Journal of Chemistry*, vol. 28, no. 2, pp. 218–222, 2004.

[7] A. Bumajdad, M. Madkour, Y. Abdel-Moneam, and M. El-Kemary, "Nanostructured mesoporous Au/TiO_2 for photocatalytic degradation of a textile dye: the effect of size similarity of the deposited Au with that of TiO_2 pores," *Journal of Materials Science*, vol. 49, no. 4, pp. 1743–1754, 2014.

[8] H. Zhang, X. Lv, Y. Li, Y. Wang, and J. Li, "P25-graphene composite as a high performance photocatalyst," *ACS Nano*, vol. 4, no. 1, pp. 380–386, 2010.

[9] T. López, M. Alvarez, F. Tzompantzi, and M. Picquart, "Photocatalytic degradation of 2,4-dichlorophenoxiacetic acid and 2,4,6-trichlorophenol with ZrO_2 and Mn/ZrO_2 sol-gel materials," *Journal of Sol-Gel Science and Technology*, vol. 37, no. 3, pp. 207–211, 2006.

[10] J.-M. Herrmann, C. Duchamp, M. Karkmaz et al., "Environmental green chemistry as defined by photocatalysis," *Journal of Hazardous Materials*, vol. 146, no. 3, pp. 624–629, 2007.

[11] Y. Tang, Z. Jiang, G. Xing et al., "Efficient Ag@AgCl cubic cage photocatalysts profit from ultrafast plasmon-induced electron transfer processes," *Advanced Functional Materials*, vol. 23, no. 23, pp. 2932–2940, 2013.

[12] Z. Zhang, C. Shao, X. Li et al., "Hierarchical assembly of ultrathin hexagonal SnS_2 nanosheets onto electrospun TiO_2 nanofibers: enhanced photocatalytic activity based on photoinduced interfacial charge transfer," *Nanoscale*, vol. 5, no. 2, pp. 606–618, 2013.

[13] D. Li, W. Wu, Y. Zhang, L. Liu, and C. Pan, "Preparation of ZnO/graphene heterojunction via high temperature and its photocatalytic property," *Journal of Materials Science*, vol. 49, no. 4, pp. 1854–1860, 2014.

[14] M. M. Uddin, M. A. Hasnat, A. J. F. Samed, and R. K. Majumdar, "Influence of TiO_2 and ZnO photocatalysts on adsorption and degradation behaviour of Erythrosine," *Dyes and Pigments*, vol. 75, no. 1, pp. 207–212, 2007.

[15] H. E. Byrne and D. W. Mazyck, "Removal of trace level aqueous mercury by adsorption and photocatalysis on silica-titania composites," *Journal of Hazardous Materials*, vol. 170, no. 2-3, pp. 915–919, 2009.

[16] A. Ye, W. Fan, Q. Zhang, W. Deng, and Y. Wang, "CdS-graphene and CdS-CNT nanocomposites as visible-light photocatalysts for hydrogen evolution and organic dye degradation," *Catalysis Science & Technology*, vol. 2, no. 5, pp. 969–978, 2012.

[17] M. Huang, C. Xu, Z. Wu, Y. Huang, J. Lin, and J. Wu, "Photocatalytic discolorization of methyl orange solution by Pt modified TiO_2 loaded on natural zeolite," *Dyes and Pigments*, vol. 77, no. 2, pp. 327–334, 2008.

[18] A. Zakersalehi, M. Nadagouda, and H. Choi, "Suppressing NOM access to controlled porous TiO_2 particles enhances the decomposition of target water contaminants," *Catalysis Communications*, vol. 41, pp. 79–82, 2013.

[19] X. Pan, M.-Q. Yang, X. Fu, N. Zhang, and Y.-J. Xu, "Defective TiO_2 with oxygen vacancies: synthesis, properties and photocatalytic applications," *Nanoscale*, vol. 5, no. 9, pp. 3601–3614, 2013.

[20] Z. Jiang, Y. Tang, Q. Tay et al., "Understanding the role of nanostructures for efficient hydrogen generation on immobilized photocatalysts," *Advanced Energy Materials*, vol. 3, no. 10, pp. 1368–1380, 2013.

[21] Y. Tang, P. Wee, Y. Lai et al., "Hierarchical TiO_2 nanoflakes and nanoparticles hybrid structure for improved photocatalytic activity," *Journal of Physical Chemistry C*, vol. 116, no. 4, pp. 2772–2780, 2012.

[22] M. Antoniadou, V. M. Daskalaki, and N. Balis, "Photocatalysis and photoelectrocatalysis using (CdS-ZnS)/TiO_2 combined photocatalysts," *Applied Catalysis B: Environmental*, vol. 107, pp. 188–196, 2011.

[23] B. Tryba, M. Piszcz, and A. W. Morawski, "Photocatalytic activity of TiO_2 - WO_3 composites," *International Journal of Photoenergy*, vol. 2009, Article ID 297319, 7 pages, 2009.

[24] Y. Peng, C. X. Liu, X. Y. Zhang, and J. H. Li, "The effect of SiO_2 on a novel CeO_2-WO_3/TiO_2 catalyst for the selective catalytic reduction of NO with NH_3," *Applied Catalysis B: Environmental*, vol. 140, pp. 276–282, 2013.

[25] M. Grätzel and R. F. Howe, "Electron paramagnetic resonance studies of doped titanium dioxide colloids," *The Journal of Physical Chemistry*, vol. 94, no. 6, pp. 2566–2572, 1990.

[26] A. Di Paola, G. Marcì, L. Palmisano et al., "Preparation of polycrystalline TiO_2 photocatalysts impregnated with various transition metal ions: characterization and photocatalytic activity for the degradation of 4-nitrophenol," *The Journal of Physical Chemistry B*, vol. 106, no. 3, pp. 637–645, 2002.

[27] Y.-K. Lai, J.-Y. Huang, H.-F. Zhang et al., "Nitrogen-doped TiO_2 nanotube array films with enhanced photocatalytic activity under various light sources," *Journal of Hazardous Materials*, vol. 184, no. 1–3, pp. 855–863, 2010.

[28] D. Wang, Z.-H. Zhou, H. Yang, K.-B. Shen, Y. Huang, and S. Shen, "Preparation of TiO_2 loaded with crystalline nano Ag by a one-step low-temperature hydrothermal method," *Journal of Materials Chemistry*, vol. 22, no. 32, pp. 16306–16311, 2012.

[29] N. Wang, T. Tachikawa, and T. Majima, "Single-molecule, single-particle observation of size-dependent photocatalytic activity in Au/TiO_2 nanocomposites," *Chemical Science*, vol. 2, no. 5, pp. 891–900, 2011.

[30] Z.-L. Ma, G.-F. Huang, D.-S. Xu, M.-G. Xia, W.-Q. Huang, and Y. Tian, "Coupling effect of la doping and porphyrin sensitization on photocatalytic activity of nanocrystalline TiO_2," *Materials Letters*, vol. 108, pp. 37–40, 2013.

[31] A.-W. Xu, Y. Gao, and H.-Q. Liu, "The preparation, characterization, and their photocatalytic activities of rare-earth-doped TiO_2 nanoparticles," *Journal of Catalysis*, vol. 207, no. 2, pp. 151–157, 2002.

[32] R. Gopalan and Y. S. Lin, "Evolution of pore and phase structure of sol-gel derived lanthana doped titania at high temperatures," *Industrial and Engineering Chemistry Research*, vol. 34, no. 4, pp. 1189–1195, 1995.

[33] H. Cai, X. Chen, Q. Li, B. He, and Q. Tang, "Enhanced photocatalytic activity from Gd, la codoped TiO_2 nanotube array photocatalysts under visible-light irradiation," *Applied Surface Science*, vol. 284, pp. 837–842, 2013.

[34] Y. B. Xie and C. W. Yuan, "Rare earth ion modified TiO_2 sols for photocatalysis application under visible light excitation," *Rare Metals*, vol. 23, no. 1, pp. 20–26, 2004.

[35] W. Wu, X. Hu, T. Xie, G. Li, and L. Zhang, "Phase structure of W-doped nano-TiO_2 produced by sol-gel method," *China Particuology*, vol. 3, no. 4, pp. 233–236, 2005.

[36] S. Yao, X. Jia, L. Jiao, C. Zhu, and Z. Shi, "La-doped TiO_2 hollow fibers and their photocatalytic activity under UV and visible light," *Indian Journal of Chemistry A*, vol. 51, no. 8, pp. 1049–1056, 2012.

[37] G. E. Mcguire, G. K. Schweitzer, and T. A. Carlson, "Study of core electron binding energies in some group IIIa, Vb, and VIb compounds," *Inorganic Chemistry*, vol. 12, no. 10, pp. 2450–2453, 1973.

[38] Y. Wang, T. Chen, and Q. Mu, "Electrochemical performance of W-doped anatase TiO_2 nanoparticles as an electrode material for lithium-ion batteries," *Journal of Materials Chemistry*, vol. 21, no. 16, pp. 6006–6013, 2011.

[39] L. J. Xiang and T. Nathan-Walleser, "Hydrothermal synthesis of W-doped titania nanofibers and its photocatalytic activity," *International Journal of Material Science*, vol. 3, pp. 104–109, 2013.

[40] V. Štengl, S. Bakardjieva, and N. Murafa, "Preparation and photocatalytic activity of rare earth doped TiO_2 nanoparticles," *Materials Chemistry and Physics*, vol. 114, no. 1, pp. 217–226, 2009.

[41] K. S. Kim and N. Winograd, "Charge transfer shake-up satellites in X-ray photoelectron spectra of cations and anions of $SrTiO_3$, TiO_2 and Sc_2O_3," *Chemical Physics Letters*, vol. 31, no. 2, pp. 312–317, 1975.

[42] C. Wen, H. Deng, J.-Y. Tian, and J.-M. Zhang, "Photocatalytic activity enhancing for TiO_2 photocatalyst by doping with La," *Transactions of Nonferrous Metals Society of China*, vol. 16, pp. s728–s731, 2006.